ADVANCED ELECTRONIC MATERIALS
www.advelectronicmat.de

Liquid-State Optoelectronics Using Liquid Metal

*Takashi Kozaki, Satoshi Saito, Yota Otsuki, Ryosuke Matsuda, Yutaka Isoda, Takuma Endo, Fumika Nakamura, Takuto Araki, Taichi Furukawa, Shoji Maruo, Masayoshi Watanabe, Kazuhide Ueno, and Hiroki Ota**

Liquid-state electronics utilizing functional liquids confined in soft templates as the sensing and actuating component present the ideal platform for enabling conformal coverage of electronic systems on curved and soft surfaces. However, to date, optoelectronic devices based on functional liquid materials as represented by photodetectors and optical memories still have not been proposed; this advancement is crucial to scaling up current liquid-state devices to a system level. Optoelectronic devices based on liquid metal and photo-switchable ionic liquid with liquid–liquid heterojunction technology are proposed. The sensing and memory schemes presented are generic for different liquid-state devices and that enables different functionality to be added to the liquid-state electronics. As a proof of concept, demonstrations are made of a light sensor composed of the ionic liquid and an optical memory using a composite of the ionic liquid and polypropylene glycol. These devices are important advancements toward the realization of liquid-state electronic systems.

Stretchable electronics, the next step beyond flexible electronics, are driven by advanced organic materials and microfabrication techniques.[1–4] They have been used for mechanically deformable devices[5–10] and sensors which enable conformal coverage of electronic systems on curved and soft surfaces. The high demand for practical applications has promoted the development of stretchable electronics in human–machine interfaces for healthcare[11–13] and soft robotics.[14] In order to add stretchability to electronic devices, conventional devices have been fabricated on an elastomer substrate to create compliant electronic systems using stretchable conductors,[15] specific wavy structural electrodes,[16] and wrinkle electrodes.[17] Liquid-state electronics based on liquid metals, gallium-based alloys, and functional liquids such as ionic liquids represent another promising platform, because a liquid naturally exhibits high deformability.

In terms of liquid-state electronics using liquid metals, potential applications that include a variety of active and passive components have been explored such as interconnects,[18] an antenna,[19] and a sensor.[20] These developments of electric components should help liquid-state electronics in taking the next step for establishment of electronic systems. However, optoelectronic devices still have not been achieved for liquid-state electronic components. Optoelectronic devices including a photoresistor[21] and photodetector[22–24] have vast applications in daily life such as optoelectronics communications[25] and environmental monitoring.[26] Various solid materials like nanowires,[27] and 2D layered materials[28] are used in optoelectronics devices as photoactive materials. In terms of liquid metals which show high deformability, it is difficult to add stable photoactive functionality to liquid metals, because by doping a photoactive component such as TiO_2 into the liquid metals, the metal liquid phase cannot be maintained. Furthermore, it is difficult to modify the surface of the liquid metals by using organic optomaterials, since the liquid surface is highly deformable.

Here, we report liquid-state optoelectronics based on liquid metal and photo-switchable ionic liquid.[29] As a proof of concept, a liquid-state light sensor and an optical memory which is switched on and off by UV and blue light exposures are demonstrated in this study. In order to realize these devices, a liquid-state heterojunction[20] was used in interconnects between sensing ionic liquid and liquid metal. The liquid-state heterojunction in the microchannels is critical to preventing intermixing of the two liquid components, especially, when the completed devices undergo mechanical deformation. These two important technologies, the photo-switchable ionic liquid and the heterojunction, achieve liquid-state optoelectronics.

For the liquid metal electrodes, we chose Galinstan. Electrodes can be fabricated by simply injecting Galinstan into microchannels. As a photo-switchable liquid material, the ionic liquid named 1-butyl-3-(4-phenylazobenzyl)imidazolium bis(trifluoromethanesulfonyl)amide ([Azo][NTf_2])[29] (**Figure 1**a) is used to realize functions as a light sensor (Figure 1b) or an optical memory (Figure 1c). Ionic liquid consists of anions and cations. Variation of their combination changes the physico-chemical properties. Azobenzene in [Azo][NTf_2]

T. Kozaki, Y. Otsuki, R. Matsuda, Y. Isoda, T. Endo, Prof. F. Nakamura, Prof. T. Araki, T. Furukawa, Prof. S. Maruo, Prof. H. Ota
Department of Mechanical Engineering
Yokohama National University
79-5 Tokiwadai, Hodogaya-ku, Yokohama 240-8501, Japan
E-mail: ota-hiroki-xm@ynu.ac.jp
S. Saito, Prof. M. Watanabe, Prof. K. Ueno
Department of Chemistry and Biotechnology
Yokohama National University
79-5 Tokiwadai, Hodogaya-ku, Yokohama 240-8501, Japan
The ORCID identification number(s) for the author(s) of this article can be found under https://doi.org/10.1002/aelm.201901135.

DOI: 10.1002/aelm.201901135

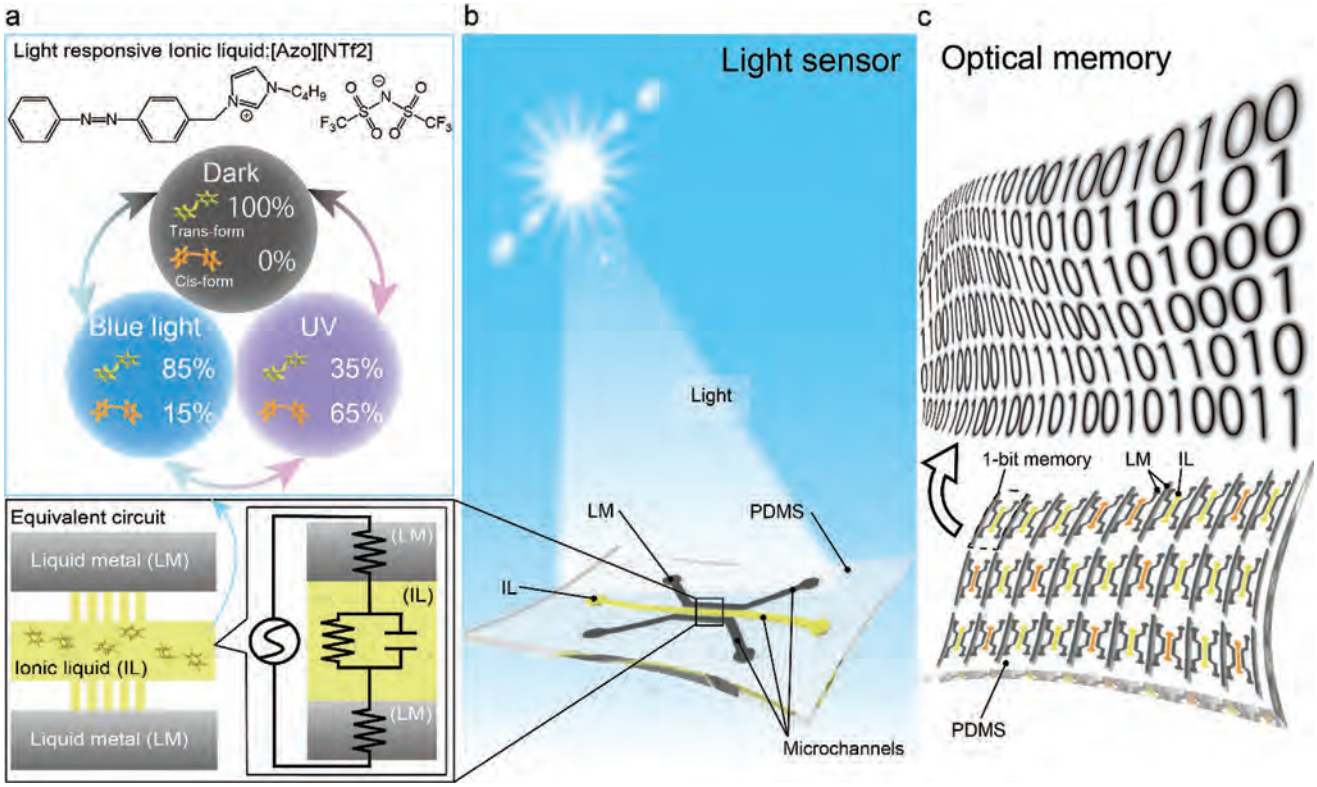

Figure 1. Images of liquid-state optoelectronic devices using liquid metal and photo-switchable ionic liquid. a) Photo-switchable functionality of the ionic liquid [Azo][NTf2]. The equivalent circuit of the device is constructed based on a Nyquist plot for sensing. b) Illustration of a liquid-state light sensor and c) a liquid-state optical memory.

is photoresponsive and can undergo a reversible isomerization controlled by light irradiation; this property is used to realize the liquid-state optoelectronics in this study. As shown in Figure 1a, azobenzene is 100% *trans*-form in the dark, and it changes to 85% *trans*-form and 15% *cis*-form on blue light exposure. On UV light exposure, the structure becomes 35% *trans*-form and 65% *cis*-form.[29] Therefore, [Azo][NTf_2] can be used as sensing material for a light sensor.

To make liquid-state devices, a liquid–liquid heterojunction obtained by microfabrication was used (Figure 1a). Generally, a liquid–liquid heterojunction is unstable, and the two liquids are immiscible. To prevent breakdown of the liquid heterointerface, we previously developed a robust heterojunction composed of liquid materials.[20] The appropriate selection of liquid materials and the architecture of the device realize the robust liquid heterointerface during fabrication as well as when the completed devices undergo mechanical deformation. The equivalent circuit (Figure 1a) of this heterojunction was established from a Nyquist plot (Figure S1, Supporting Information). Based on the equivalent circuit, the light sensor and optical memory were developed (Figure 1b,c).

As shown in Figure S2, Supporting Information, a light sensor was fabricated by a soft lithography technique. The architecture concept we followed has been previously described.[20] Briefly, to prevent the ionic liquid and liquid metal from mixing when the latter was injected or when the device was deformed, we implemented high flow resistance structures of 30 µm wide channels at the interface of the two liquids for liquid–liquid heterojunction. **Figure 2**a shows the developed device. To observe the functionality of light sensing, the equivalent circuit in Figure 1a was determined from a Nyquist plot (Figure S1, Supporting Information). In the case of our light sensor, the resistance value could be obtained from the resistance at 2000 Hz. As shown in Figure 2b and Figure S3, Supporting Information, the resistances of the developed light sensor decrease with respect to UV or blue light intensity. The decrease is caused by increase of the ion mobility. Penetration efficiency of light is almost 0% in this device, since the molar extinction coefficient of [Azo][NTf_2] is 2600 M^{-1} cm^{-1}; that is, based on a calculation, the light can reach only into a 5 µm layer on the surface. The unbalance of density of *cis*- and *trans*-forms in an ionic liquid leads to increase of ion mobility by convective flow of ions (Supporting Information 1 and Figure S4, Supporting Information). Eventually, the resistance decreases by light exposure, since resistance is determined by ion mobility and number which is not altered during light exposure. Figure 2c shows the relationship between intensity of UV or blue lights and resistance. Standard deviations were calculated from the five samples, and error bars were indicated. The light intensity measurement might not be strongly affected since the error is small considering the range of light intensity the device can detect. In the case of UV light, the obtained sensitivity of this light sensor is 21 Mohm mW^{-1} mm^{-2}, and the device sensitivity to UV light is higher than that to blue light. The sensitivity at 370 nm wave length is the highest among the 370–630 nm light sources based on the frequency characteristic results (Figure 2d). This is related to the absorption spectrum of

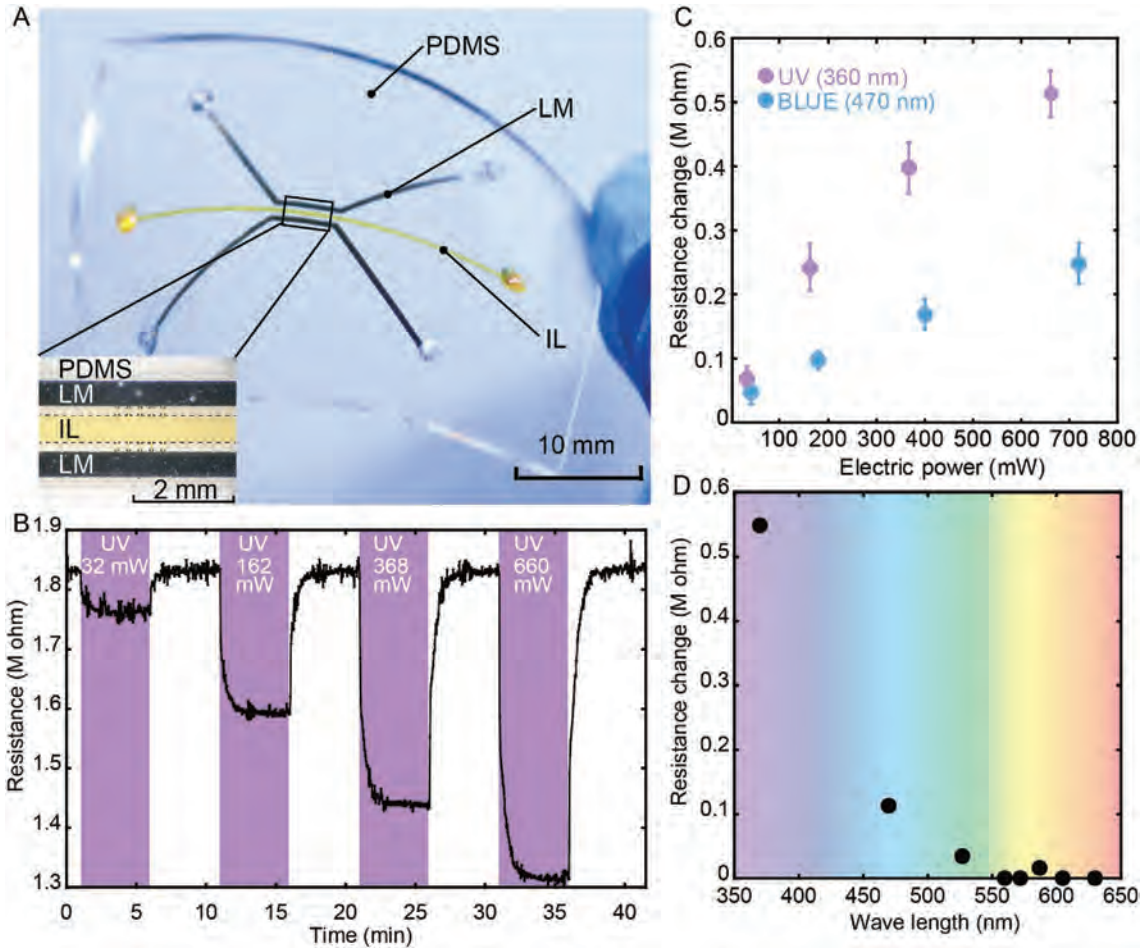

Figure 2. Experimental characterization of the light sensor. a) The developed light sensor. b) Resistance change during UV exposure at 32, 162, 368, and 660 mW. c) The relationship between resistance change of the developed device and electric power for UV (370 nm) and blue LED (470 nm). d) Wave length characteristics of resistance change during light exposure.

the ionic liquid [Azo][NTf_2] (Figure S5, Supporting Information) and it is why the sensitivity in the UV spectrum which is related to energy absorption from light is higher in the UV range. The intensities of signals might depend on the cross-sectional area of the heterojunction channels. However, based on previous work,[20] the width of the heterojunction channels should be less than 250 µm because of a limitation in the fabrication process. We know that signals can be acquired using 30 µm width heterojunction channels. Considering the widths of the main channels for the ionic liquid and Galinstan channels, the minimum size of the sensing part would likely be around 700 µm in length and 50 µm in width with a reasonable signal to noise ratio being maintained. In order to achieve this minimum size, the fabrication process without soft-lithography should be revised in a future work.

Noise might occur in the wiring between the device and impedance analyzer. In order to decrease this noise, a certain voltage must be applied by the impedance analyzer (Figure S6, Supporting Information). The applied voltage should be decided based on the requirement for sensitivity of the light intensity and the energy efficiency. In addition, the impedance of the devices is affected by temperature (Figure S7a, Supporting Information); that is to say, the ion mobility increases and ion dissociation (generation) is enhanced with respect to the temperature.[20] However, the resistance change becomes larger linearly as a function of the light intensity regardless of temperature (Figure S7b,c, Supporting Information). This is why it might be possible to adjust the resistance change at each temperature based on the calibration curve of a light sensor at each temperature by using another temperature sensor as shown in ref. [30].

As our second application in liquid-state optoelectronics, we developed an optical memory (**Figure 3**a). The basic mechanism taking advantage of the photoisomerization in [Azo][NTf_2] was the same as that of the light sensor. However, in the case of an optical memory, the resistance change after UV or blue light exposure must be maintained for a limited time period as shown in Figure 3a. In the case of a light sensor, the resistance should return to the basal value in the dark as soon as the light exposure stops. Indeed, the resistance of the light sensor returns to the standard value as soon as the light is turned off, since the amount of the converted *cis*-form is small, and it diffuses into the ionic liquid as explained in Supporting Information 1. In order to ensure the memory effect, we increased light transmission of the liquid electrolyte by mixing polypropylene glycol (PPG) with

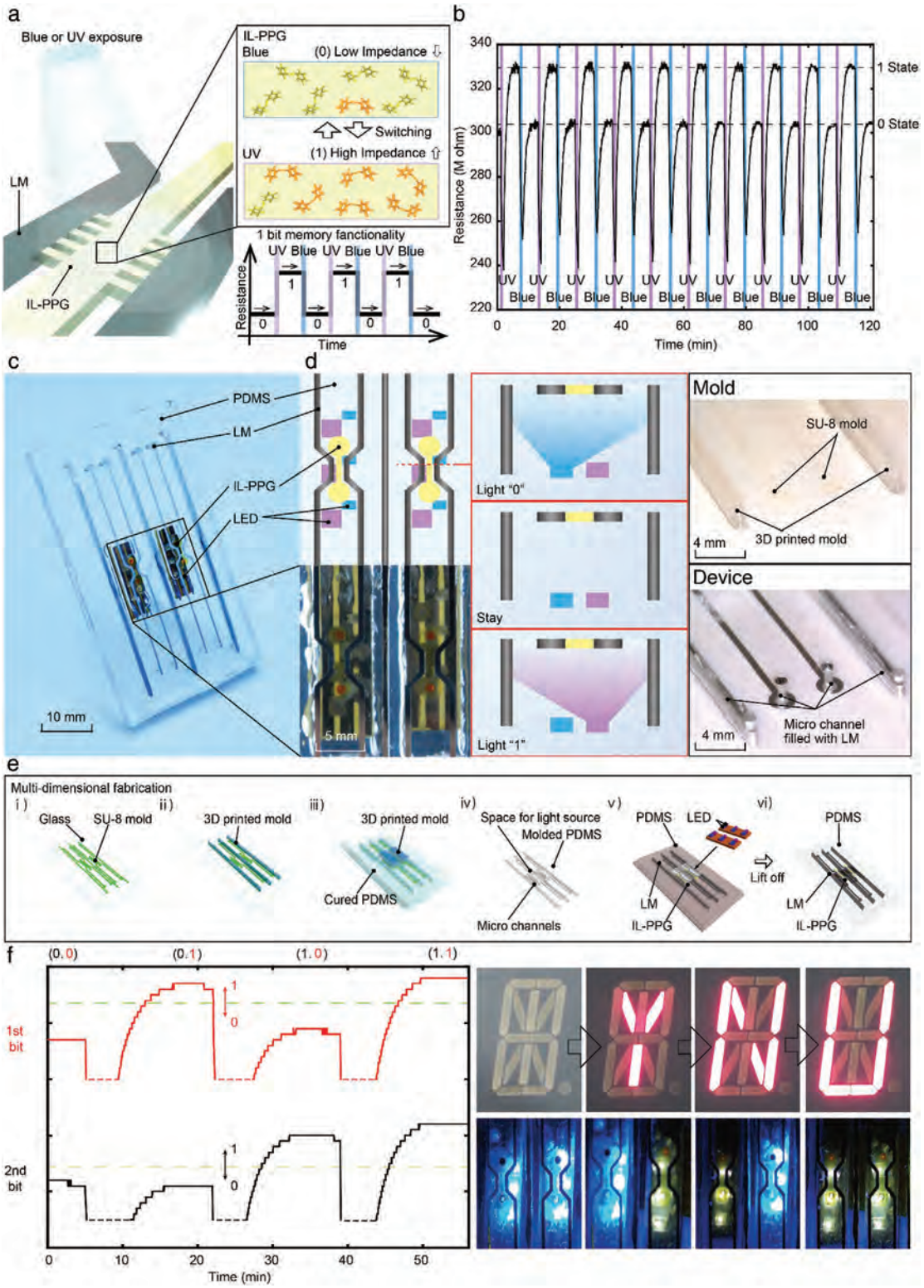

Figure 3. Demonstration of the liquid-state optical memory. a) Image and mechanism schematic of the liquid-state optical memory. b) Resistance changes and is maintained after 300 s exposure to UV or blue light. The device exhibits memory-like functionality by switching between UV light and blue light. Optical image of the developed two 1-bit optical memories. d) Two LED arrays for switching phase transition of the IL-PPG are fixed in PDMS substrate of the devices. e) Fabrication process flow of the device. f) The digital display is controlled by two 1-bit liquid-state optical memories.

the ionic liquid. Dilution of the ionic liquid allows the conversion to *cis*-form for most azobenzene molecules of [Azo][NTf_2] in the bulk liquid electrolyte, and therefore, the resistance retains a constant value for a long time after light exposure.

The device was fabricated basically by soft lithography (Figure S8, Supporting Information). For switching resistivity of the device by UV and blue lights, a UV light array or a blue LED array was used as a light source. A mixture of [Azo][NTf_2] and PPG (IL-PPG) was injected into one microchannel and the liquid metal was injected into another. After the injection, the LED array was inserted into the space. Using this developed device, we investigated the characteristics of the 1-bit memory functionality. The Nyquist plot (Figure S9, Supporting Information) was measured using a potentiostat, which determined the frequency indicating the real resistance part in the device. In the device, the frequency was 100 Hz. As shown in Figure S10, Supporting Information, the resistance of [Azo][NTf_2] returned to the standard resistance value when exposed for more than 60 s to blue light with a power greater than 720 mW. On the other hand, the resistance of [Azo][NTf_2] was saturated after exposure for more than 60 s to UV light with a power greater than 660 mW. The resistance change might be associated with the ion mobility that was changed by UV or blue light. Azobenzene is converted to *cis*-form by UV light exposure, and its polarity makes intermolecular bonds stronger. On the other hand, it is returned to *trans*-form by blue light exposure and becomes nonpolar, which decreases the ion mobility by weakening intermolecular bonds. This is why the resistance might be controlled through ion mobility by switching UV or blue light. Right before the resistance change by UV and blue light, the resistance decreased for a short time. This might be because the LED array fixed onto the device generated a slight amount of heat during light exposure, and that increased the ion mobility. Figure 3b shows repeatability of the liquid-state optical memory using these parameters. In terms of resistance retention, the resistance with UV light exposure (660 mW for 60 s) decreases 1.5% after 90 min (Figure S11, Supporting Information).

As a demonstration of memory functionality of our device, we developed a digital display system as shown in Figure 3c,d. In this demonstration, we fabricated the device with two of our 1-bit liquid-state optical memories on a chip with UV and blue light sources (Figure 3c,d). In order to set a series of the liquid-state memories into one system chip, it was crucial to prevent light in one memory from exposing the other memory. As shown in Figure 3d, 3D printed channels filled with liquid metal were added on both sides of each memory, which acted as "walls" to prevent light from affecting the neighbor memory. The fabrication process is shown in Figure 3e. The digital display system was set up as shown in Figure S12, Supporting Information, which showed "Y", "N", and "U" on 16 segments according to signals from the device. The system determined "0" or "1" based on whether the resistance of each bit memory was lower or higher than a threshold value of resistance (Figure S13, Supporting Information). "Y", "N", and "U" displays, composed of 16 segments, were decided depending on a combination of "1" and "0". As shown in Figure 3f, one 1-bit memory is not affected by the other 1-bit memory. The threshold value was 182 Mohm in this device. Using this system, we successfully carried out the display control of "Y", "N", and "U". The memory functionality of our liquid-state optical memory was demonstrated.

In this paper, we have proposed liquid-state optoelectronic devices using liquid metal and photo-switchable ionic liquid. As demonstrations, a light sensor and an optical memory were developed. Our devices could potentially be developed into highly deformable and stretchable optoelectronics based on functional liquid materials using other structures and materials. Such devices could be used advantageously for advanced wearable electronics having integrated circuits and for soft robotics including memory functionality. Currently, a variety of issues, including the sensitivity and response time of the light sensing, still must be resolved before practical devices can be developed. However, the work presents an important step toward the potential realization of liquid-state electronic systems that offer new form factors and functionality.

Experimental Section

Synthesis of [Azo][NTf2]: Synthesis of [Azo][NTf_2] was done according to the literature procedure.[29] Briefly, there were four processes in the synthesis: firstly, nitrosobenzene (4.70 mmol) (Tokyo Chemical Industry Co., Ltd.), 12 mL of acetic acid, and p-toludidine (4.70 mmol) (FUJIFILM Wako Pure Chemical Corporation) were mixed. 4-Methyl azobenzene was purified through a recrystallization process. Secondly, *N*-bromosuccinimide (3.60 mmol) (FUJIFILM Wako Pure Chemical Corporation), benzoyl peroxide (0.21 mmol) (Sigma-Aldrich Co., Ltd.), and 150 mL of carbon tetrachloride (FUJIFILM Wako Pure Chemical Corporation) were mixed, and exposed to UV light. Carbon tetrachloride was removed from the solution. 4-(Bromomethyl)azobenzene was purified through a recrystallization process. Thirdly, 1-buthyl-3-(4-phenyazobenezyl) imidazoliumbromide ([Azo]Br) was synthesized. 4-(Bromomethyl)azobenzene (1.31 mmol), 1-butylimidazole (1.38 mmol) (Sigma-Aldrich Co., Ltd.), and 120 mL of ethanol were mixed in a nitrogen gas flow for 12 h. [Azo]Br was collected after evaporation of ethanol. [Azo]Br was purified through a recrystallization process. Finally, 1-butyl-3-(4-phenylazobenzyl)imidazolium bis(trifluoromethanesulfonyl)amide ([Azo][NTf_2]) was synthesized by dripping an aqueous solution of Li[NTf_2] (1.20 mmol)(Morita Chemical Industries Co., Ltd.) into the mixture of [Azo]Br (1.00 mmol) in water (100 mL).

Light Sensor Fabrication: A light sensor was fabricated based on the soft lithography technique. Photoresist, SU-8 (SU-83050, Nippon Kayaku Co., Ltd), was coated on the glass substrate. Next, the SU-8 substrate was exposed to UV light. The patterned substrate was baked at 95 °C for 1 min. The mold was obtained by removing the unexposed area using SU-8 developer (Nippon Kayaku Co., Ltd.) (Figure S2a, Supporting Information).Liquid PDMS was poured onto the mold, and cured by heating at 70 °C for 3 h (Figure S2b, Supporting Information). The cured PDMS block was peeled off (Figure S2c, Supporting Information). Simultaneously, a 50 µm PDMS membrane was bonded chemically using an excimer lamp (L12530-01, Hamamatsu Photonics K.K.) (Figure S2e, Supporting Information). Liquid metal (Galinstan, Zairyo-ya.com) and ionic liquids were injected into microchannels (Figure S2g, Supporting Information). Finally, the developed device was obtained by peeling it from the glass substrate (Figure S2h, Supporting Information).

Optical Memory Fabrication: The mold fabrication was based on the multi-dimensional microfabrication combined with optical fiber lithography[31] and soft lithography. The mold of the optical memory was composed of microchannels for electrodes and the sensing part in the device and 3D printed channels to prevent undesired light irradiation to a neighbor 1-bit memory as shown in Figure 3. The mold of the microchannels was fabricated by the photo-lithography method (Figure 3e(i)). Then, the 3D printed channels were additionally fabricated using an optical fiber (Figure 3e(ii)).

Each 3D printed channel was designed with a height of 2 mm, a width of 1 mm, and a length of 52.5 mm (longitudinal direction). The mold was fabricated by optical fiber lithography with an optical fiber having 1 mm core diameter (FT1000UMT, Thorlabs Inc.), equipped with a dispenser robot (IMAGE MASTER 350PC Smart XMΩX, Musashi Engineering, Inc.). A UV laser (CUBE 375-16C, Coherent Inc.) was used for a light source to cure the photopolymer. Using the mold, liquid metal was injected into microchannels to act as electrodes, and then the IL-PPG (polypropylene glycol diol type 3000, FUJIFILM Wako Pure Chemical Corporation) (10 wt%, 90 wt%) as sensing liquid was injected. The LED array composed of blue and UV LEDs was inserted into the space. PDMS was poured around the LED array space and cured (Figure 3e(v)). The developed device was obtained by peeling it from the glass substrate (Figure 3e(vi)).

Analysis of the Nyquist Plot: The Nyquist plot was measured at an applied DC bias of 0 V, with a 10 mV AC voltage superimposed by a potentiostat (Modulab XM ECS, Solartron Analytical). The measurement frequency ranged from 100 Hz to 1 MHz for [Azo][NTf2], and from 10 Hz to 1 MHz for the IL-PPG. A model of electrolyte resistance R and double layer capacitance C in series was used based on the Nyquist plot.

Light Exposure for the Sensor: To measure the light intensity dependence of the sensor, the fabricated device was put in a thermostatic chamber (SU-242, ESPEC Corp.) at 25 °C. LEDs were used to expose the device from the top. The resistances were measured when the irradiation intensities of the UV and blue LED light sources were changed to 4, 6, 8, and 10 V. In terms of other wave lengths, light was irradiated at 10 V to the device.

Demonstration of the Optical Memory: The fabricated device was placed in a thermostatic chamber set at 25 °C as shown in Figure S12, Supporting Information. For the demonstration of the liquid-state optical memory, the digital display system was realized, which showed "Y", "N", and "U" on a 16-segment LED display according to the combination of input signals from the liquid-state optical memory. A PC read the resistance data of the device from a potentiostat, and converted the resistance data to the logical value based on whether resistance was low or high compared to a threshold value. A pulse generator (GS820, Yokogawa Electric Corp.) read the logical value in the PC, and generated the actual driving voltage based on the logical value. As shown in Figure S13, Supporting Information, the 2-bit decode circuit selected a 1-bit identifying signal in the four 1-bit signals based on a combination of the logical values. The 16-segment LED drive circuit in the system drove an appropriate segment in the 16-segment LED display for showing "Y", "N", or "U" based on the identifying signal.

Supporting Information

Supporting Information is available from the Wiley Online Library or from the author.

Acknowledgements

This work was supported by the Japan Science and Technology Agency, PRESTO (Grant Number JPMJPR18J2), Takeda Science Foundation, Life Science Research Grants. MIC/SCOPE (Number: 181603007) and research grants from KIOXIA Corporation (former Toshiba Memory Corporation). H.O. acknowledges support from a Grant-in-Aid for Young Scientists (A) and Grant-in-Aid for Challenging Exploratory Research provided by the Japan Society for the Promotion of Science. S. M. acknowledges support from the Cross-Ministerial Strategic Innovation Promotion Program (SIP) to construct the optical fiber lithography system, and thanks CMET Inc. for providing the photopolymer (TSR-883).

Conflict of Interest

The authors declare no conflict of interest.

Keywords

ionic liquid, liquid metal, optoelectronics

Received: October 14, 2019
Revised: January 14, 2020
Published online:

[1] N. Lu, C. Lu, S. Yang, J. Rogers, *Adv. Funct. Mater.* **2012**, *22*, 4044.
[2] S. Gong, W. Schwalb, Y. Wang, Y. Chen, Y. Tang, J. Si, B. Shirinzadeh, W. Cheng, *Nat. Commun.* **2014**, *5*, 3132.
[3] M. Amjadi, Y. J. Yoon, I. Park, *Nanotechnology* **2015**, *26*, 375501.
[4] C. Wang, D. Hwang, Z. Yu, K. Takei, J. Park, T. Chen, B. Ma, A. Javey, *Nat. Mater.* **2013**, *12*, 899.
[5] D. J. Lipomi, M. Vosgueritchian, B. C. K. Tee, S. L. Hellstrom, J. A. Lee, C. H. Fox, Z. Bao, *Nat. Nanotechnol.* **2011**, *6*, 788.
[6] W. Gao, H. Ota, D. Kiriya, K. Takei, A. Javey, *Acc. Chem. Res.* **2019**, *52*, 523.
[7] L.-C. Tai, W. Gao, M. Chao, M. Bariya, Q. P. Ngo, Z. Shahpar, H. Y. Y. Nyein, H. Park, J. Sun, Y. Jung, E. Wu, H. M. Fahad, D.-H. Lien, H. Ota, G. Cho, A. Javey, *Adv. Mater.* **2018**, *30*, 1707442.
[8] Y. Gao, H. Ota, E. W. Schaler, K. Chen, A. Zhao, W. Gao, H. M. Fahad, Y. Leng, A. Zheng, F. Xiong, C. Zhang, L.-C. Tai, P. Zhao, R. S. Fearing, A. Javey, *Adv. Mater.* **2017**, *29*, 1701985.
[9] H. Ota, M. Chao, Y. Gao, E. Wu, L.-C. Tai, K. Chen, Y. Matsuoka, K. Iwai, H. Fahad, W. Gao, H. Y. Y. Nyein, L. Lin, A. Javey, *ACS Sens.* **2017**, *2*, 990.
[10] W. Gao, H. Y. Y. Nyein, Z. Shahpar, L.-C. Tai, E. Wu, M. Bariya, H. Ota, H. M. Fahad, K. Chen, A. Javey, *IEEE IEDM Technical Digest*, IEEE, Piscataway, NJ **2016**, pp. 6.6.1–6.6.2.
[11] G. Schwartz, B. C. K. Tee, J. Mei, A. L. Appleton, D. H. Kim, H. Wang, Z. Bao, *Nat. Commun.* **2013**, *4*, 1858.
[12] T. Yamada, Y. Hayamizu, Y. Yamamoto, Y. Yomogida, A. Izadi-Najafabadi, D. N. Futaba, K. Hata, *Nat. Nanotechnol.* **2011**, *6*, 296.
[13] S. Park, S. W. Heo, W. Lee, D. Inoue, Z. Jiang, K. Yu, H. Jinno, D. Hashizume, M. Sekino, T. Yokota, K. Fukuda, K. Tajima, T. Someya, *Nature* **2018**, *561*, 516.
[14] W. Hu, G. Z. Lum, M. Mastrangeli, M. Sitti, *Nature* **2018**, *554*, 81.
[15] T. Sekitani, N. Yoshiaki, K. Hata, F. Takanori, A. Takuzo, T. Someya, *Science* **2008**, *321*, 1468.
[16] R. C. Webb, A. P. Bonifas, A. Behnaz, Y. Zhang, K. J. Yu, H. Cheng, M. Shi, Z. Bian, Z. Liu, Y. S. Kim, W. H. Yeo, J. S. Park, J. Song, Y. Li, Y. Huang, A. M. Gorbach, J. A. Rogers, *Nat. Mater.* **2013**, *12*, 938.
[17] S.-J. Park, J. Kim, M. Chu, M. Khine, *Adv. Mater. Technol.* **2016**, *1*, 1600053.
[18] S. Harada, T. Arie, S. Akita, K. Takei, *Adv. Electron. Mater.* **2015**, *1*, 1500080.
[19] J. H. So, J. Thelen, A. Qusba, G. J. Hayes, G. Lazzi, M. D. Dickey, *Adv. Funct. Mater.* **2009**, *19*, 3632.
[20] H. Ota, K. Chen, Y. Lin, D. Kiriya, H. Shiraki, Z. Yu, T. J. Ha, A. Javey, *Nat. Commun.* **2014**, *5*, 5032.
[21] A. A. Bakulin, R. Lovrincic, X. Yu, O. Selig, H. J. Bakker, Y. L. A. Rezus, P. K. Nayak, A. Fonari, V. Coropceanu, J. L. Brédas, D. Cahen, *Nat. Commun.* **2015**, *6*, 7880.
[22] M. Kim, P. Kang, J. Leem, S. W. Nam, *Nanoscale* **2017**, *9*, 4058.
[23] S. Park, K. Fukuda, M. Wang, C. Lee, T. Yokota, H. Jin, H. Jinno, H. Kimura, P. Zalar, N. Matsuhisa, S. Umezu, G. C. Bazan, T. Someya, *Adv. Mater.* **2018**, *30*, 1802359.
[24] W. Wu, X. Wang, X. Han, Z. Yang, G. Gao, Y. Zhang, J. Hu, Y. Tan, A. Pan, C. Pan, *Adv. Mater.* **2019**, *31*, 1805913.

[25] T. Gu, N. Petrone, J. F. McMillan, A. Van Der Zande, M. Yu, G. Q. Lo, D. L. Kwong, J. Hone, C. W. Wong, *Nat. Photonics* **2012**, *6*, 554.
[26] Z. Ran, X. Wang, Y. Li, D. Yang, X. G. Zhao, K. Biswas, D. J. Singh, L. Zhang, *npj Comput. Mater.* **2018**, *4*, 1.
[27] C. M. Lieber, J. F. Wang, M. S. Gudiksen, X. F. Duan, Y. Cui, *Science* **2001**, *293*, 1455.
[28] F. Xia, H. Wang, Y. Jia, *Nat. Commun.* **2014**, *5*, 4458.
[29] C. Wang, X. Ma, Y. Kitazawa, Y. Kobayashi, S. Zhang, H. Kokubo, M. Watanabe, *Macromol. Rapid Commun.* **2016**, *37*, 1960.
[30] W. Gao, S. Emaminejad, H. Y. Y. Nyein, S. Challa, K. Chen, A. Peck, H. Fahad, H. Ota, S. Hiroshi, D. Kiriya, D. H. Lien, G. A. Brooks, R. W. Davis, A. Javey, *Nature* **2016**, *529*, 509.
[31] T. Ibi, E. Komada, T. Furukawa, S. Maruo, *Microfluid. Nanofluid.* **2018**, *22*, 69.

